Research Square

Preprints are preliminary reports that have not undergone peer review.
They should not be considered conclusive, used to inform clinical practice,
or referenced by the media as validated information.

Pan-cancer multi-omics profiling and single-cell characterization of KCNAB2 identify a proliferative blast state in acute myeloid leukemia with in vitro functional validation

Jianhua Zhu
H uazhong University of Science and Technology
Qianhe Xu
Hubei University of Chinese Medicine
Shuhong Ke
keshu1980@aliyun.com

H uazhong University of Science and Technology

Research Article

Keywords: KCNAB2, pan-cancer, acute myeloid leukemia, tumor immune microenvironment

Posted Date: November 19th, 2026

DOI: https://doi.org/10.21203/rs.3.rs-11345010/v1

License: This work is licensed under a Creative Commons Attribution 4.0 International License.
Read Full License

Additional Declarations: No competing interests reported.

Pan-cancer multi-omics profiling and single-cell characterization of KCNAB2 identify a proliferative blast state in acute myeloid leukemia with in vitro functional validation

Jianhua Zhu[1,†], Qianhe Xu[2,†], Shuhong Ke[3,*]

1. Department of Laboratory Medicine, Wuhan No.1 Hospital, Tongji Medical College, Huazhong University of Science and Technology, No.215 Zhongshan Avenue, Wuhan，Hubei, 430030, China

2.School of Laboratory Medicine, Hubei University of Chinese Medicine, No. 16 West Huangjia Lake Road, Wuhan 430065, Hubei, P.R. China

3. Department of Endocrinology, Wuhan No.1 Hospital, Tongji Medical College, Huazhong University of Science and Technology, No.215 Zhongshan Avenue, Wuhan，Hubei, 430030, China

† *These authors contributed equally to this work.*

* Correspondence: Shuhong Ke, Department of Endocrinology, Wuhan No.1 Hospital, Wuhan Hubei, 430030, China; E-mail: keshu1980@aliyun.com

Abstract:

Background/Objectives: KCNAB2, a voltage-gated potassium channel β-subunit, has been implicated in tumorigenesis, but its specific role in acute myeloid leukemia (AML) remains unclear. This study aimed to profile KCNAB2 across human cancers and delineate its regulatory function in AML cell proliferation and apoptosis.

Methods: Public databases (GEPIA2.0, UALCAN, LinkedOmics) were used to profile KCNAB2 across cancers as a background analysis (expression, copy number variation, DNA methylation, immune infiltration, tumor mutational burde

n, microsatellite instability, stemness and drug sensitivity), which supported the subsequent AML-focused work. KCNAB2 expression was examined at single-cell resolution in an adult AML cohort (GSE116256) and validated in an independent pediatric AML cohort (GSE154109). CCK-8, EdU and apoptosis assays assessed KCNAB2 function in AML cell lines in vitro.

Results: KCNAB2 was heterogeneously expressed and significantly upregulated in AML and several solid tumors. Copy number variation and DNA methylation drove its dysregulation, and expression correlated with immune infiltration and checkpoint markers. Single-cell profiling localized KCNAB2 to the malignant, progenitor-like compartment of AML in both cohorts. In the pediatric cohort, KCNAB2-positive blasts were characterized by cell-cycle and DNA-replication programs, whereas the adult cohort showed no gene-level significance and only a preliminary calcium-signaling enrichment. Knockdown of KCNAB2 significantly suppressed proliferation and induced apoptosis in AML cells.

Conclusions: KCNAB2 modulates proliferative and apoptotic phenotypes in AML, and its expression is associated with immune and oncogenic transcriptional programs, supporting its role as a functional regulator and a candidate therapeutic target requiring further preclinical validation.

Keywords: KCNAB2; pan-cancer; acute myeloid leukemia; tumor immune microenvironment

1. Introduction

Cancer remains a leading cause of mortality worldwide, with substantial heterogeneity in molecular pathogenesis, clinical behavior and therapeutic response across tumor types [1,2]. Immunotherapy has transformed treatment paradigms for several malignancies, but only a subset of patients derives durable benefit, underscoring the need for robust biomarkers and novel therapeutic vulnerabilities [3–6]. Potassium channels, traditionally studied for their roles in cellular excitability and ion homeostasis, have emerged as important contributors to cancer bi

ology [7,8]. Their dysregulation is frequently observed in malignancies and has been associated with tumor progression, metastasis and patient outcomes [9]. B eyond ion conduction, potassium channel subunits participate in proliferation, m igration, apoptosis and modulation of the tumor immune microenvironment [10, 11], making them attractive candidates for both biomarker and therapeutic deve lopment.

KCNAB2, localized to chromosome 1p36, encodes the KVβ2 auxiliary protein that modulates the biophysical properties of voltage-gated potassium channel α subunits [12,13]. It also possesses aldo-keto reductase activity, suggesting metab olic and signaling functions beyond channel modulation [14]. KCNAB2 has bee n implicated in several malignancies, including colorectal cancer [15], lymphom a [16] and pituitary tumors [17]. In lung adenocarcinoma, it is downregulated and associated with poor prognosis and immune infiltration deficiency [18], wit h FTO-mediated m6A methylation identified as an upstream regulator [19]. The se observations point to a context-dependent role for KCNAB2 across cancer t ypes, but also raise a practical question: which tumor type offers the clearest f unctional handle on this gene?

AML is a compelling setting to address this question. First, KCNAB2 is upreg ulated in AML and its knockdown has been reported to suppress proliferation and promote apoptosis [25], providing an initial functional anchor that can be extended. Second, AML is a disease in which single-cell resolution is essential, because blast heterogeneity and the proportion of cycling cells directly affect disease behavior and treatment response. Third, the proliferative state of AML blasts is a clinically meaningful axis, and any gene that marks or supports it i s a plausible therapeutic target. However, the cellular state with which KCNAB 2 associates at single-cell resolution, and whether such associations generalize a cross independent AML cohorts, remain unexplored. Critically, KCNAB2's trans criptional effects and its relationship to the cycling blast compartment in AML

have not been defined.

To address these gaps, we designed a study in which pan-cancer multi-omics analysis serves primarily as a backdrop for AML-focused functional work. We first profiled KCNAB2 across cancers to establish its expression landscape, genomic and epigenetic regulation, immune associations and drug-sensitivity patterns, using these analyses to determine whether KCNAB2 behaves in a tumor-type-specific manner and to justify the choice of AML as the focus. We then centered the study on AML: single-cell characterization in an adult cohort (GSE116256) and an independent pediatric cohort (GSE154109), followed by siRNA-mediated knockdown in AML cell lines to test the functional consequences of KCNAB2 loss. This structure keeps the pan-cancer work in a supporting role and places the AML-specific findings — single-cell localization and the proliferation/apoptosis phenotype — at the center of the study. Together, these analyses define KCNAB2 as a marker of a proliferative blast state in AML and a candidate target for further preclinical testing.

2. Materials and Methods

2.1. Expression Analysis of KCNAB2 in Cancers

The GEPIA2.0 database (http://gepia2.cancer-pku.cn) are used to perform a pan-cancer analysis of KCNAB2 mRNA expression. KCNAB2 protein expression profiles across distinct cancer types were quantified using the UALCAN online analytical platform (https://ualcan.path.uab.edu/index.html). Pan-cancer tumor-vs-normal mRNA differences were also visualized using the Sangerbox 3.0 platform (Fig. 1A).

2.2. Tumor Stage and Prognosis Analysis of KCNAB2 in Cancers

The GEPIA2.0 database ("pathological stage plot" and "survival" module) is applied to evaluate the tumor stage and the prognostic value of KCNAB2 in pan-cancer.

2.3. Correlation Analyses of KCNAB2 Expression with Immune Cell Infiltration, Tumor Mutational Burden, Microsatellite Instability and Stemness

The Sangerbox 3.0 platform (http://www.sangerbox.com, "Pan-cancer analysis" module) is used to perform all these correlation analyses.

2.4. Enrichment Analysis of the Gene Co-Expression Network for KCNAB2

We used the LinkedOmics database to select the RNA-seq data types of AML patients from the TCGA database and used the statistical method of Pearson Correlation test to obtain other genes related to the target genes. GO and KEGG enrichment analyses were performed in the DAVID database (https://david.ncifcrf.gov/). GO enrichment analysis included biological processes (BP), cellular components (CC), and molecular functions (MF). KEGG analysis could identify the neighbor genes and pathways associated with KCNAB2.

2.5. Copy Number Variation (CNV), Methylation and Drug Sensitivity

The GSCA database was used to analyze CNV, methylation and drug sensitivity of KCNAB2 in pan-cancer and their associations with gene expression. Drug-sensitivity correlations were derived from the GDSC and CTRP databases (via Sangerbox 3.0).

2.6. Single-Cell Analysis of KCNAB2 Gene Expression

We analyzed KCNAB2 expression in GSE116256 using author-annotated cell types and normal/malignant predictions. KCNAB2 positivity was defined as UMI > 0. Violin plots of log1p(UMI) and positivity fractions were generated across 22 cell types by status. Malignant versus normal expression was compared across six hematopoietic lineages using two-sided Wilcoxon rank-sum tests with Benjamini–Hochberg FDR (significance: FDR < 0.05 and < 0.001). For independent validation we used GSE154109 (19 samples, 29,330 cells). Because author-provided diagnostic labels were unavailable, samples were assigned to pediatric AML, pediatric ALL or control bone marrow using marker-module scores (B-lymphoid, myeloid, blast-like, progenitor-like, T-cell) and GEO sample ordering; only the eight pediatric AML samples were retained, and analyses were restricted to myeloid, blast-like and progenitor-like cells. Cells were classified as KCNAB2-positive when ≥1 KCNAB2 UMI was detected.

2.7. Differential Expression Between KCNAB2-Positive and KCNAB2-Negative Blasts

For each single-cell cohort, counts were aggregated to pseudo-bulk profiles defined by sample and KCNAB2 status, and differential expression was tested with

DESeq2 using a design containing sample and, where malignant-subset composition was available, subset proportions as covariates. Genes with FDR-adjusted $P < 0.05$ were considered significant. Gene set enrichment analysis was performed with fgsea against KEGG annotations obtained from org.Hs.eg.db, with significance set at FDR-adjusted $P < 0.05$.

2.8. Cell Culture and Transfection

AML cell lines (U937, NB4) were obtained from the American Type Culture Collection. Cells were cultured in RPMI-1640 medium (Invitrogen, Carlsbad, CA, USA) supplemented with 10% fetal bovine serum (FBS, Invitrogen) in a humidified atmosphere containing 5% CO2 at 37°C. To silence KCNAB2 expression, small interfering RNA (siRNA) specific to KCNAB2 and a control siRNA were obtained from Ruibo (China). Transfection of siRNA into cells was performed using Lipofectamine® 3000 reagent (Thermo Fisher, USA).

2.9. Quantitative Real-Time PCR

TRIzol reagent (Invitrogen, USA) served as the lysis buffer for total RNA isolation from cultured cells. After reverse transcription of extracted RNA, qPCR amplification was carried out to determine the transcript abundance of genes of interest. Normalization was achieved using GAPDH as the housekeeping reference, and relative quantification was performed via the $2^{-\Delta\Delta Ct}$ computational method. Primer sequences employed in this study are listed below: KCNAB2 forward:5′-TGACCCACGTCATCAACCAG-3′ KCNAB2 reverse: 5′-ACCTCCACTTTCTCACGCTG-3′
GAPDH forward: 5′-GGATTTGGTCGTATTGGGCG-3′
GAPDH reverse: 5′-CGGTGCCATGGAATTTGCC-3′

2.10. Cell Counting Kit-8 (CCK-8)

The cell proliferation was determined using CCK-8 assay (DoJinDo, Shiga, Jap

an). The transfected cells were (1.0×10^3 cells per well) were plated into 96 well plates. After incubation for 0, 24, 48 and 72 hours, 10ul of CCK-8 solution was added and incubated for 2 h. Absorbance at 450 nm was measured using a microplate reader (Thermo Fisher, USA).

2.11. EdU Assay

EdU assay was performed according to the instructions of BeyoClick™ EdU Cell Proliferation Kit (Beyotime, Shanghai, China). Cells were incubated with EdU solution for 2 h. Subsequent to wash the cells twice with PBS, cells were fixed with 4% para formaldehyde for 20 min. Then, cells were treated with 0.5% Triton X-100 solution for 10 min. After washing with PBS once, add the staining solution and incubate for 30 min. Wash twice for 5min each with 0.5% Triton X-100 solution. The cell nucleus was stained with 1×DAPI for 15 min. After washed twice with PBS, the cells were examined and captured on camera using fluorescence microscopy.

2.12. Apoptosis Assay

AML cells were resuspended and washed twice with 1 mL of cold PBS. After centrifugation, cells were resuspended in 1×Annexin V Binding Buffer (prepared by 1:4 dilution of the stock solution with deionized water) at a concentration of 1×10^6 cells/mL. A 250 μL aliquot of the cell suspension was incubated with 5 μL of Annexin V-AbFluor™ 488 (Abbkine, KAT0002, China) for 15 minutes at room temperature in the dark. Subsequently, 5 μL of propidium iodide (PI) was added, followed by 500 μL of PBS. The apoptosis of cells was analyzed by flow cytometry (Beckman Coulter DxFLEX).

2.13. Statistical Analysis

SPSS version 21.0 served as the statistical analysis platform for the in vitro experiments. All data originate from a minimum of three biologically independent experiments and are expressed as means ± standard deviation. Differences between groups were determined using Student's t-test or one-way analysis of variance (ANOVA). Statistical significance was considered at $p<0.05$. Bioinformatics and single-cell analyses were performed in R (v4.6.1). Correlations with immune infiltration, TMB, MSI, stemness and drug sensitivity used Spearman or Pearson correlation with Benjamini–Hochberg FDR control across cancer types. Single-cell malignant-versus-normal comparisons used two-sided Wilcoxon rank-sum tests with Benjamini–Hochberg FDR adjustment (significance: FDR < 0.05). Differential expression between KCNAB2-positive and KCNAB2-negative cells was tested on sample-level pseudo-bulk profiles with DESeq2, using a design containing sample and malignant-subset proportions as covariates; genes with FDR-adjusted $P < 0.05$ were considered significant. Gene set enrichment was performed with fgsea against KEGG annotations (org.Hs.eg.db), with significance set at FDR-adjusted $P < 0.05$; nominal results are explicitly labeled as such. Differences in cell-subset composition were tested by chi-square tests.

3. Results

3.1. Pan-Cancer Expression of KCNAB2

We investigated KCNAB2 expression in both normal and various tumor tissues. mRNA expression of KCNAB2 was significantly upregulated in ESCA, STES, STAD, SKCM, PAAD, LAML, PCPG, and CHOL compared with adjacent normal tissues (Fig. 1A). GEPIA2.0 validation confirmed KCNAB2 upregulation in LAML, ESCA, SKCM, STAD, PAAD, and PCPG (Fig. 1B). At the protein level, KCNAB2 was markedly elevated in HNSC, RCC, PAAD, a

nd OV, but decreased in GBM, LUAD, UCEC, and HCC (Fig. 1C). Furthermo re, higher KCNAB2 expression positively correlated with advanced clinical stag es in BLCA, LUAD, KICH, and THCA (Fig. 1D).

3.2. Pan-Cancer Prognostic Value of KCNAB2

To elucidate the association of the KCNAB2 expression with the prognosis in cancers, we investigated the prognostic significance of KCNAB2 expression lev els in multiple cancers. Forest plots revealed that elevated KCNAB2 mRNA ex pression was associated with worse overall survival (OS) in LAML, KIPAN, S KCM-M, COAD, and COADREAD (Fig. 2A), as well as shorter disease-free s urvival (DFS) in COAD, COADREAD, KIPAN, and SKCM-M (Fig. 2B). Kapl an-Meier analyses corroborated that high KCNAB2 expression conferred unfavo rable OS in COAD, COADREAD, GBM, LAML, SKCM-M, and KIPAN, whe reas low expression predicted poor outcomes in GBMLGG (Fig. 2C). Similarly, GEPIA2.0 survival curves confirmed shorter OS in LAML and COAD patient s with high KCNAB2 expression, while lower expression predicted reduced OS in LUAD (Fig. 2D).

3.3. Correlations of KCNAB2 Expression with CNV and DNA Methylation

To explore the upstream regulatory mechanisms of KCNAB2, copy number var iations (CNVs) were analyzed using GSCA. Frequent CNVs were observed in OV, CHOL, KICH, PCPG, ESCA, UCS, SARC, LUSC, LUAD, ACC, and LI HC, but were rare in LAML, PRAD, THYM, and THCA (Fig. 3A). Heterozyg ous amplifications predominantly occurred in OV, UCS, SARC, LUAD, and C ESC, whereas heterozygous deletions prevailed in KICH, CHOL, BRCA, REA

D, LIHC, and LUSC (Fig. 3B). Homozygous amplifications were frequent in E SCA, OV, UCS, and PAAD, while homozygous deletions were predominantly enriched in DLBC, ACC, and LIHC (Fig. 3C). Notably, CNV levels positively correlated with KCNAB2 mRNA expression in SARC, PCPG, and KICH (Fig. 3D). DNA methylation analysis identified prominent differential methylation lev els of KCNAB2 in KIRC, COAD, UCEC, LIHC, and BRCA (Fig. 3E). KCNA B2 promoter methylation negatively correlated with its mRNA expression in S KCM, THYM, LGG, KIRP, THCA, and COAD (Fig. 3F).

3.4. KCNAB2 in the Tumor Immune Microenvironment

We evaluated KCNAB2 expression versus immune infiltration. KCNAB2 positiv ely correlated with CD8+ T cells, M1/M2 macrophages, and memory CD4+ T cells across tumors, but negatively with plasma cells, mast cells, and dendritic cells (Fig. 4A). Significant correlations occurred with CD8+ T cells (31 cancer s), CD4+ T cells (18), B cells (29), monocytes (33), DCs (31), and macrophag es (37) (Fig. 4B). KCNAB2 also correlated with immunostimulators, immunoin hibitors, MHC molecules, chemokines, and receptors in most cancers; negative correlations with MHC molecules and immunostimulators (TNFRSF14, TNFRSF 19, CD80, CD86, IL2RA) appeared in LGG and GBMLGG (Fig. 4C). Immune checkpoint analysis showed positive correlations in most cancers, but negative correlations with inhibitory (IL10, PDCD1, LAG3, TGFB1, VEGFA, VEGFB) and stimulatory (CD28, ITGB2, ICAM1, CD80, CCL5) ICP genes in LGG and GBMLGG (Fig. 4D).

3.5. Relationship Between KCNAB2 Expression and Response to Immunotherapy and Stemness

We next analyzed clinical markers of immunotherapy responsiveness. KCNAB2 expression positively correlated with tumor mutational burden (TMB) in SKCM, but inversely in LAML and STAD (Fig. 5A). Microsatellite instability (MSI) positively correlated with KCNAB2 in GBMLGG, but negatively in STES, KIPAN, STAD, TGCT, and DLBC (Fig. 5B). Neoantigen load displayed divergent patterns, showing a weak positive correlation in PRAD but negative correlations in KIRC, MESO, and BLCA (Fig. 5C). Homologous recombination deficiency (HRD) positively correlated with KCNAB2 in COAD, COADREAD, BRCA, SARC, PRAD, and BLCA, but negatively in GBM, LUSC, THYM, and UVM (Fig. 5D). Stemness analysis revealed that KCNAB2 expression positively correlated with DNA stemness score (DNAss) in THCA, but negatively across 14 other cancer types (Fig. 5E). Similarly, RNA stemness score (RNAss) was inversely associated with KCNAB2 in 23 cancers, yet positively linked in GBMLGG, LGG, THYM, and SKCM (Fig. 5F).

3.6. Analysis of KCNAB2-Related Genes in AML

To explore KCNAB2-mediated oncogenic mechanisms in acute myeloid leukemia (AML), co-expressed genes were identified using LinkedOmics (Fig. 6A–C). Functional enrichment of the top 100 KCNAB2-associated genes (identified via LinkedOmics TCGA-LAML and annotated using DAVID) revealed GO terms enriched in actin cytoskeleton organization, small GTPase-mediated signal transduction, protein binding, kinase activity, and transferase activity (Fig. 6D–F). KEGG pathway analysis highlighted involvement in Yersinia infection, chemokine signaling, leukocyte transendothelial migration, and ubiquitin-mediated proteolysis (Fig. 6G).

3.7. Correlation Between KCNAB2 and Drug Sensitivity

Pan-cancer drug response profiling in GDSC and CTRP databases demonstrated significant correlations between KCNAB2 expression and drug sensitivity. In GDSC, high KCNAB2 expression predicted increased sensitivity to Lapatinib, Erlotinib, and XAV939, but resistance to Methotrexate, I-BET-762, and BHG712 (Fig. 7A). In CTRP, KCNAB2 positively correlated with sensitivity to JW-55, ML312, and BRD-K99006945, while inversely correlating with belinostat, BRD-K30748066, and LRRK2-IN-1 (Fig. 7B).

3.8. Single-Cell Expression of KCNAB2 and Characterization in an Independent Pediatric AML Cohort

To characterize KCNAB2 at single-cell resolution, we analyzed GSE116256 (van Galen et al., 2019; 41,089 cells). KCNAB2 was detected in only 12.0% of all 41,089 cells (median 1 UMI) — 18.4% of malignant versus 7.9% of normal cells (Fig. 8A) — and was concentrated in myeloid progenitors and monocytes and lowest in lymphoid and erythroid lineages (Fig. 8B). Malignant cells expressed more KCNAB2 than normal cells (mean log1p 0.149 vs. 0.061, Wilcoxon $P<2.2\times10^{-16}$), and malignant cells exceeded their normal counterparts across all six lineages at the single-cell level (two-sided Wilcoxon rank-sum test on individual cells with Benjamini-Hochberg correction; significant for HSC, Prog, Mono, cDC and GMP, whereas ProMono was not significant, FDR=0.179) (Fig. 8C). In this adult cohort, KCNAB2-positive versus KCNAB2-negative malignant cells (paired pseudo-bulk DESeq2) yielded no gene at FDR<0.05; only calcium signaling was enriched (hsa04020, NES =1.51, adjusted $P=4.3\times10^{-3}$) (Fig. 8D). In an independent pediatric cohort (GSE154109; eight samples, 11,180 myeloid, blast-like and progenitor-like cells; 30.1% KCNAB2-positive), 260 genes differed (185 up-regulated) with cell-cycle and DNA-replication enrichment (hsa0

4110: NES=2.27, adjusted P=8.7×10^{-8}; hsa03030: NES =2.31, adjusted P=9.1×10^{-6}; leading edge: CDK1, CCNA2, CCNB1, PLK1, MCM2–7, PCNA) (Fig. 8E–G). Thus, KCNAB2 is enriched in the malignant, progenitor-like compartment of AML in both cohorts. In pediatric disease, KCNAB2 positivity marks a proliferative blast state; in adults, the only signal was a preliminary calcium-signaling enrichment without gene-level significance. This difference may reflect distinct driver spectra, cycling blast proportions, and the lower KCNAB2 detection rate in adults (12.0% vs 30.1%).

3.9. Experimental Validation in AML Cell Lines

We then examined effects of KCNAB2 on the proliferation and apoptosis in AML cell. The expression of KCNAB2 in cells was knocked down using siRNA. The mRNA level of KCNAB2 is decreased by specific siRNA against KCNAB2 (Fig. 9A). KCNAB2 knockdown significantly reduced cell proliferation as determined by CCK-8 assay and EdU assay (Fig. 9B, C). Furthermore, KCNAB2 knockdown significantly increased the AML cell apoptosis (Fig. 9D).

4. Discussion

KCNAB2 shows heterogeneous expression across malignancies. It is upregulated in ESCA, gastric adenocarcinoma, SKCM, PAAD and AML, but downregulated in LUAD [18]. This context-dependent pattern may reflect differences in cellular origin, oncogenic drivers and microenvironment, and possibly its dual identity as a potassium channel auxiliary subunit and an aldo-keto reductase [14,20]. This heterogeneity argues against a single, tumor-agnostic function for KCNAB2 and supports a disease-specific investigation, which is why the functional work here focused on AML.

CNV and DNA methylation emerge as likely drivers of KCNAB2 dysregulation. Heterozygous amplifications predominate in OV, sarcoma and LUAD, where

as deletions are common in KICH, CHOL and BRCA; CNV correlates positively with KCNAB2 expression in sarcoma and KICH, while promoter methylation correlates inversely in SKCM, THYM, LGG and THCA. Together with FTO-mediated m6A suppression of KCNAB2 in NSCLC [19], these findings point to convergent DNA- and RNA-level regulation. Prognostic direction is also cancer type-specific: high expression predicts poor outcomes in AML, COAD and SKCM, whereas low expression predicts unfavorable prognosis in LUAD [18]. In AML, KCNAB2-associated genes enrich for chemokine signaling, leukocyte transendothelial migration and cytoskeletal regulation, suggesting a role in leukemic trafficking and bone marrow microenvironment interactions rather than a purely proliferative program.

KCNAB2 expression correlates with immune infiltration and checkpoint markers across cancers, but these are associative findings: whether KCNAB2 shapes the immune microenvironment or is co-regulated with it remains undetermined. The inverse KCNAB2–TMB association in LAML, in particular, is consistent with AML's low mutational burden and suggests that KCNAB2 reflects a cell-state program rather than mutational load. We therefore focused the functional work on the cell-intrinsic role of KCNAB2 in AML.

The pan-cancer, single-cell and in vitro analyses address different layers of KCNAB2 biology. Bulk multi-omics defines the landscape of KCNAB2 dysregulation and identifies immune, cytoskeletal and chemokine-related associations. Single-cell analysis localizes KCNAB2 to the malignant, progenitor-like compartment in both cohorts. The siRNA experiments establish that KCNAB2 loss impairs proliferation and promotes apoptosis, providing causal evidence for a functional role. These layers are not expected to converge on one pathway: bulk co-expression captures averaged tumor-level associations, single-cell positivity captures a cell-state correlation, and knockdown captures a phenotypic consequence. Importantly, the proliferative signature in pediatric blasts is directionally consistent

with the anti-proliferative effect of knockdown, which strengthens the link between the observational and causal arms of the study.

The single-cell results provide the most direct link between KCNAB2 and AML cell state. In the pediatric cohort, KCNAB2-positive blasts were distinguished by a coordinated cell-cycle and DNA-replication program (260 genes at FDR < 0.05; leading edge CDK1, CCNA2, CCNB1, PLK1, MCM2-7, PCNA), indicating that KCNAB2 positivity marks a proliferative rather than quiescent blast state. This is directionally consistent with the anti-proliferative effect of knockdown, and together the two observations suggest that KCNAB2 supports the cycling fraction of AML blasts. In the adult cohort, no individual gene passed FDR correction and only calcium signaling was nominally enriched (hsa04020; NES =1.51, adjusted P=0.004); we therefore treat this result as hypothesis-generating. The difference is mechanistically plausible: pediatric AML is dominated by primitive, rapidly cycling blasts, so the KCNAB2-positive subpopulation naturally captures a cycling compartment, whereas the adult contrast was drawn within malignant cells. These two observations are complementary rather than contradictory, but they are not equivalent in strength.

The association between KCNAB2 positivity and a proliferative blast state carries therapeutic implications. If KCNAB2 marks or contributes to the cycling fraction of AML blasts, targeting it could preferentially affect this compartment. This remains speculative: the single-cell comparison cannot distinguish whether KCNAB2 drives proliferation or is merely co-expressed with proliferation programs. Cell-cycle profiling and rescue experiments after knockdown are required to resolve this. Nevertheless, the convergence of pan-cancer immune associations, single-cell localization to the progenitor-like compartment, and a causal anti-proliferative phenotype positions KCNAB2 as a candidate therapeutic target in AML and provides a framework for testing it in patient-derived models.

This study has several limitations. First, it relies mainly on public transcriptomic data, and drug-sensitivity associations from GDSC/CTRP cell-line panels require validation in patient-derived models. Second, KCNAB2 was detected in only a minority of AML cells, and positivity was defined by detection (UMI > 0) rather than quantitative expression; sensitivity analyses with a stricter threshold (UMI ≥ 2) supported the same direction, but full per-cell quantification will require deeper sequencing. Third, the pediatric cohort comprised only eight samples with exploratory, marker-based diagnostic assignment, so those results should be regarded as hypothesis-generating rather than definitive. Fourth, functional validation was limited to siRNA knockdown in two cell lines (U937, NB4), without rescue, overexpression or in vivo models; whether KCNAB2 acts through its aldo-keto reductase activity or via PI3K/AKT/mTOR therefore remains open. These limitations define the scope of the present findings and the experiments needed to test them further.

Conclusions

This study integrates pan-cancer multi-omics profiling with single-cell characterization and in vitro validation to define the role of KCNAB2 in AML. KCNAB2 is aberrantly expressed across cancers, localizes to the malignant, progenitor-like compartment of AML, and marks a proliferative blast state in pediatric disease. siRNA-mediated knockdown suppresses proliferation and promotes apoptosis in AML cell lines, providing causal evidence that KCNAB2 supports AML cell proliferation and survival. These findings position KCNAB2 as a candidate therapeutic target in AML and provide a framework for testing its function in patient-derived and in vivo models.

Abbreviations

TMB tumor mutation burden

MSI microsatellite instability

OS overall survival

DFS disease-free survival

RCC Renal cell carcinoma

LUAD Lung adenocarcinoma

NSCLC Non-small cell lung cancer

ACC Adrenocortical carcinoma

BLCA Bladder urothelial carcinoma

BRCA Breast invasive carcinoma

CHOL Cholangiocarcinoma

COAD Colon adenocarcinoma

ESCA Esophageal carcinoma

HNSC Head and neck squamous cell carcinoma

KICH Kidney chromophobe

KIRC Kidney renal clear cell carcinoma

KIRP Kidney renal papillary cell carcinoma

LIHC Liver hepatocellular carcinoma

LUSC Lung squamous cell carcinoma

MESO Mesothelioma

PAAD Pancreatic adenocarcinoma

PRAD Prostate adenocarcinoma

READ Rectum adenocarcinoma

STAD Stomach adenocarcinoma

THCA Thyroid carcinoma

SKCM Skin cutaneous melanoma

GBM Glioblastoma multiforme

UCS Uterine Carcinosarcoma

TGCT Testicular germ cell tumors

Authors' Contributions

Conceptualization, S.K.; Methodology, J.Z. and Q.X.; Software, J.Z.; Validation,

J.Z. and Q.X.; Formal Analysis, J.Z. and Q.X.; Investigation, J.Z. and Q.X.; Resources, S.K.; Data Curation, J.Z. and Q.X.; Writing – Original Draft Preparation, J.Z.; Writing – Review & Editing, J.Z., Q.X. and S.K.; Visualization, J.Z.; Supervision, S.K.; Project Administration, S.K. All authors have read and agreed to the published version of the manuscript.

Funding

This research received no external funding.

Ethics Approval and Consent to Participate

Not applicable. This study relied exclusively on publicly available, de-identified databases (The Cancer Genome Atlas [TCGA] and the Gene Expression Omnibus [GEO]) accessed through GEPIA2.0, UALCAN, LinkedOmics, GSCA and Sangerbox. No human subjects, patient samples, or animal experiments were involved.

Consent for Publication

Not applicable.

Availability of Data and Materials

The public datasets analyzed in this study are available from the Gene Expression Omnibus (accessions GSE116256 and GSE154109) and The Cancer Genome Atlas (TCGA) via the portals cited in the Methods. Specifically, the TCGA-LAML cohort was used in this study. The in vitro experimental data generated in this study are available from the corresponding author upon reasonable request.

Competing Interests

All authors declare that they have no competing interests.

Acknowledgements

The authors thank the data generators and the maintainers of the public resources used in this study, including The Cancer Genome Atlas (TCGA), the Gene Expression Omnibus (GEO), GEPIA2.0, UALCAN, LinkedOmics, GSCA and Sangerbox.

References

[1] Sung, H.; Filho, A.M.; Laversanne, M.; et al. Global Cancer Statistics 2024: GLOBOCAN Estimates of Incidence and Mortality Worldwide for 34 Cancers in 186 Countries. CA Cancer J. Clin. 2026, 76, e70090. https://doi.org/10.3322/caac.70090.

[2] Chen, S.; Cao, Z.; Prettner, K.; et al. Estimates and Projections of the Global Economic Cost of 29 Cancers in 204 Countries and Territories from 2020 to 2050. JAMA Oncol. 2023, 9, 465-472. https://doi.org/10.1001/jamaoncol.2022.7826.

[3] Havel, J.J.; Chowell, D.; Chan, T.A. The Evolving Landscape of Biomarkers for Checkpoint Inhibitor Immunotherapy. Nat. Rev. Cancer 2019, 19, 133-150. https://doi.org/10.1038/s41568-019-0116-x.

[4] Bagaev, A.; Kotlov, N.; Nomie, K.; et al. Conserved Pan-Cancer Microenvironment Subtypes Predict Response to Immunotherapy. Cancer Cell 2021, 39, 845-865.e7. https://doi.org/10.1016/j.ccell.2021.04.014.

[5] Li, T.; Fan, J.; Wang, B.; et al. TIMER: A Web Server for Comprehensive Analysis of Tumor-Infiltrating Immune Cells. Cancer Res. 2017, 77, e108-e110. https://doi.org/10.1158/0008-5472.CAN-17-0307.

[6] Charoentong, P.; Finotello, F.; Angelova, M.; et al. Pan-Cancer Immunogenomic Analyses Reveal Genotype-Immunophenotype Relationships and Predictors of Response to Checkpoint Blockade. Cell Rep. 2017, 18, 248-262. https://doi.o

rg/10.1016/j.celrep.2016.12.019.

[7] Comes, N.; Bielanska, J.; Vallejo-Gracia, A.; et al. The Voltage-Dependent K(+) Channels Kv1.3 and Kv1.5 in Human Cancer. Front. Physiol. 2013, 4, 283. https://doi.org/10.3389/fphys.2013.00283.

[8] Ko, E.A.; Kim, Y.W.; Lee, D.; et al. Expression of Potassium Channel Genes Predicts Clinical Outcome in Lung Cancer. Korean J. Physiol. Pharmacol. 2019, 23, 529-537. https://doi.org/10.4196/kjpp.2019.23.6.529.

[9] Van, N.T.H.; Nam, J.H. Intermediate Conductance Calcium-Activated Potassium Channel (KCa3.1) in Cancer: Emerging Roles and Therapeutic Potentials. Biochem. Biophys. Res. Commun. 2024, 733, 150605. https://doi.org/10.1016/j.bbrc.2024.150605.

[10] Xu, P.; Mo, X.; Xia, R.; et al. KCNN4 Promotes the Progression of Lung Adenocarcinoma by Activating the AKT and ERK Signaling Pathways. Cancer Biomark. 2021, 31, 187-201. https://doi.org/10.3233/CBM-201045.

[11] Chen, S.; Su, X.; Mo, Z. KCNN4 Is a Potential Biomarker for Predicting Cancer Prognosis and an Essential Molecule That Remodels Various Components in the Tumor Microenvironment: A Pan-Cancer Study. Front. Mol. Biosci. 2022, 9, 812815. https://doi.org/10.3389/fmolb.2022.812815.

[12] Yee, J.X.; Rastani, A.; Soden, M.E. The Potassium Channel Auxiliary Subunit Kvβ² (Kcnab2) Regulates Kv1 Channels and Dopamine Neuron Firing. J. Neurophysiol. 2022, 128, 156-168. https://doi.org/10.1152/jn.00194.2022.

[13] Perkowski, J.J.; Murphy, G.G. Deletion of the Mouse Homolog of KCNAB2, a Gene Linked to Monosomy 1p36, Results in Associative Memory Impairments and Amygdala Hyperexcitability. J. Neurosci. 2011, 31, 46-54. https://doi.org/10.1523/JNEUROSCI.2634-10.2011.

[14] Luo, D.; et al. Expression of AKRs Superfamily and Prognostic in Human Gastric Cancer. Medicine 2023, 102, e33041. https://doi.org/10.1097/MD.0000000000033041.

[15] Garate, J.; Maimó-Barceló, A.; Bestard-Escalas, J.; et al. A Drastic Shift in Lipid Adducts in Colon Cancer Detected by MALDI-IMS Exposes Alteration

s in Specific K(+) Channels. Cancers 2021, 13, 1350. https://doi.org/10.3390/cancers13061350.

[16] Tu, J.; Kuang, Z.; Xie, X.; et al. Prognostic and Predictive Value of a mRNA Signature in Peripheral T-Cell Lymphomas: A mRNA Expression Analysis. J. Cell. Mol. Med. 2021, 25, 84-95. https://doi.org/10.1111/jcmm.15851.

[17] Ashton, C.; Rhie, S.K.; Carmichael, J.D.; Zada, G. Role of KCNAB2 Expression in Modulating Hormone Secretion in Somatotroph Pituitary Adenoma. J. Neurosurg. 2020, 134, 787-793. https://doi.org/10.3171/2019.12.JNS192435.

[18] Lyu, Y.; Wang, Q.; Liang, J.; Zhang, L.; Zhang, H. The Ion Channel Gene KCNAB2 Is Associated with Poor Prognosis and Loss of Immune Infiltration in Lung Adenocarcinoma. Cells 2022, 11, 3438. https://doi.org/10.3390/cells11213438.

[19] Li, Y.; Niu, J.; Sun, Z.; Liu, J. FTO-Mediated m6A Methylation of KCNAB2 Inhibits Tumor Property of Non-Small Cell Lung Cancer Cells and M2 Macrophage Polarization by Inactivating the PI3K/AKT Pathway. J. Biochem. Mol. Toxicol. 2025, 39, e70232. https://doi.org/10.1002/jbt.70232.

[20] Cheng, F.; Tang, Y.F.; Cao, Y.; et al. KCNAB2 Overexpression Inhibits Human Non-Small-Cell Lung Cancer Cell Growth in Vitro and in Vivo. Cell Death Discov. 2023, 9, 382. https://doi.org/10.1038/s41420-023-01679-5.

[21] Baharom, F.; Ramirez-Valdez, R.A.; Khalinzehazd, A.; et al. Systemic Vaccination Induces CD8(+) T Cells and Remodels the Tumor Microenvironment. Cell 2022, 185, 4317-4332.e15. https://doi.org/10.1016/j.cell.2022.10.006.

[22] Speiser, D.E.; Chijioke, O.; Schaeuble, K.; Munz, C. CD4(+) T Cells in Cancer. Nat. Cancer 2023, 4, 317-329. https://doi.org/10.1038/s43018-023-00521-2.

[23] Thorsson, V.; Gibbs, D.L.; Brown, S.D.; et al. The Immune Landscape of Cancer. Immunity 2018, 48, 812-830.e14. https://doi.org/10.1016/j.immuni.2018.03.023.

[24] Fetsch, V.; Schwöbel, L.; Ozyerli-Goknar, E.; et al. Menin Inhibition Enhances Graft-Versus-Leukemia Effects by T-Cell Activation and Endogenous Retr

ovirus Induction in AML. Blood 2026, 147, 584-601. https://doi.org/10.1182/blood.2025029712.

Figure legend

Figure 1. The expression levels of KCNAB2 in pan-cancer.

(**A**) KCNAB2 expression levels in different cancers from the TCGA database analyzed by the Sangerbox database. (**B**) KCNAB2 expression levels in different cancers and paired normal tissue in the GEPIA database. (**C**) KCNAB2 protein levels in different cancers in the UALCAN database. (**D**) KCNAB2 expression levels in different tumor stages in GEPIA2.0 database. (*p<0.05; **p<0.01; *** p<0.001; **** p<0.0001).

Figure 2. The prognosis value of KCNAB2 in pan-cancer.

(**A**, **B**) The forest plot indicated the correlations of KCNAB2 with overall survival (OS) and disease-free survival (DFS) in pan-cancer. (**C**, **D**) Kaplan-Meier analysis of the association between KCNAB2 expression and OS.

Figure 3. The CNV and DNA methylation of KCNAB2 in pan-cancer.

(**A**) The change frequency of CNV in KCNAB2 was showed by GSCA database. (**B-C**) The analysis of the Heterozygous/Homozygous CNV of KCNAB2 in pan-cancer. (**D**)The correlation of CNV with KCNAB2 mRNA expression in pan-cancer. (**E**) The differential methylation analysis of KCNAB2 in pan-cancer. (**F**) The correlation analysis showed that the methylation level of KCNAB2 was negatively correlated with mRNA expression

Figure 4. Correlation of KCNAB2 with the tumor immune microenvironment pan-cancer.

Relationship of KCNAB2 expression with immune cell infiltration analysis in pan-cancer by (**A**) CIBERSORT method, (**B**) xCELL method. (**C**, **D**) Relationshi

p of KCNAB2 expression with immune-related genes and immune checkpoint g enes. (*p<0.05)

Figure 5. Relationship of KCNAB2 expression with TMB, MSI, Neoantigen, HRD, and cancer stemness in pan-cancer.

(**A**) Correlation between KCNAB2 expression and TMB. (B) Correlation betw een KCNAB2 expression and MSI. (**C**) Correlation between KCNAB2 expressi on and neoantigen. (**D**) Correlation between KCNAB2 expression and HRD. (**E**) Correlation between KCNAB2 expression and tumor stemness based on DNA methylation (DNAss). (**F**) Correlation between KCNAB2 expression and tumor stemness based on gene expression (RNAss).

Figure 6. The analyses of KCNAB2-related genes in AML. (A) Genes with significantly high correlation with KCNAB2 in the LAML cohort. Heatmaps sh owing the enrichment patterns of the top 100 genes positively (50) (**B**) or neg atively (50) (**C**) correlated with KCNAB2 expression of LAML in TCGA data base. (**D**-**F**) The GO enrichment analysis was applied with the top 100 KCNA B2 positive related genes. (**G**) The KEGG enrichment analysis was used to an alyze the top 100 KCNAB2 positive related genes.

Figure 7. Drug sensitivity analysis based on KCNAB2 expression using the two different databases GDSC (A) and CTRP (B).

Figure 8. Single-cell KCNAB2 expression and KCNAB2-positive versus KC NAB2-negative comparison in adult and pediatric AML. (A) KCNAB2-positi ve cells among normal (n = 23,004) and malignant (n = 16,169) cells in GSE 116256; dashed line, 12.0% overall; P, two-proportion z-test. (B) KCNAB2-posi tive fraction by cell type (GSE116256). (C) Mean log1p(KCNAB2) for normal versus malignant cells across six lineages; Wilcoxon FDR (*FDR<0.05, **FDR < 0.001, ns=not significant). (D) GSEA for hsa04020 calcium signaling in adul

t AML (NES =1.51, adjusted P=4.3×10^{-3}). (E) Volcano plot of KCNAB2-positi ve versus KCNAB2-negative cells in GSE154109 (30.1% positive); red points, FDR<0.05 (n=260). (F) GSEA for hsa04110 cell cycle (NES=2.27, adjusted P= 8.7×10^{-8}). (G) Top enriched KEGG pathways ranked by adjusted P (GSE15410 9); red bars, adjusted P < 0.05; dashed line, P=0.05.

Figure 9. The biological functions of KCNAB2 in AML. (A) Relative mRN A expression of KCNAB2 in AML cells transfected with KCNAB2 siRNA. (B, C) Cell proliferation of AML cell was detected by CCK8 assay and EdU ass ay. (D) The apoptosis of AML cell was assessed by flow cytometry analysis. *p<0.05, **p<0.01.

Figures

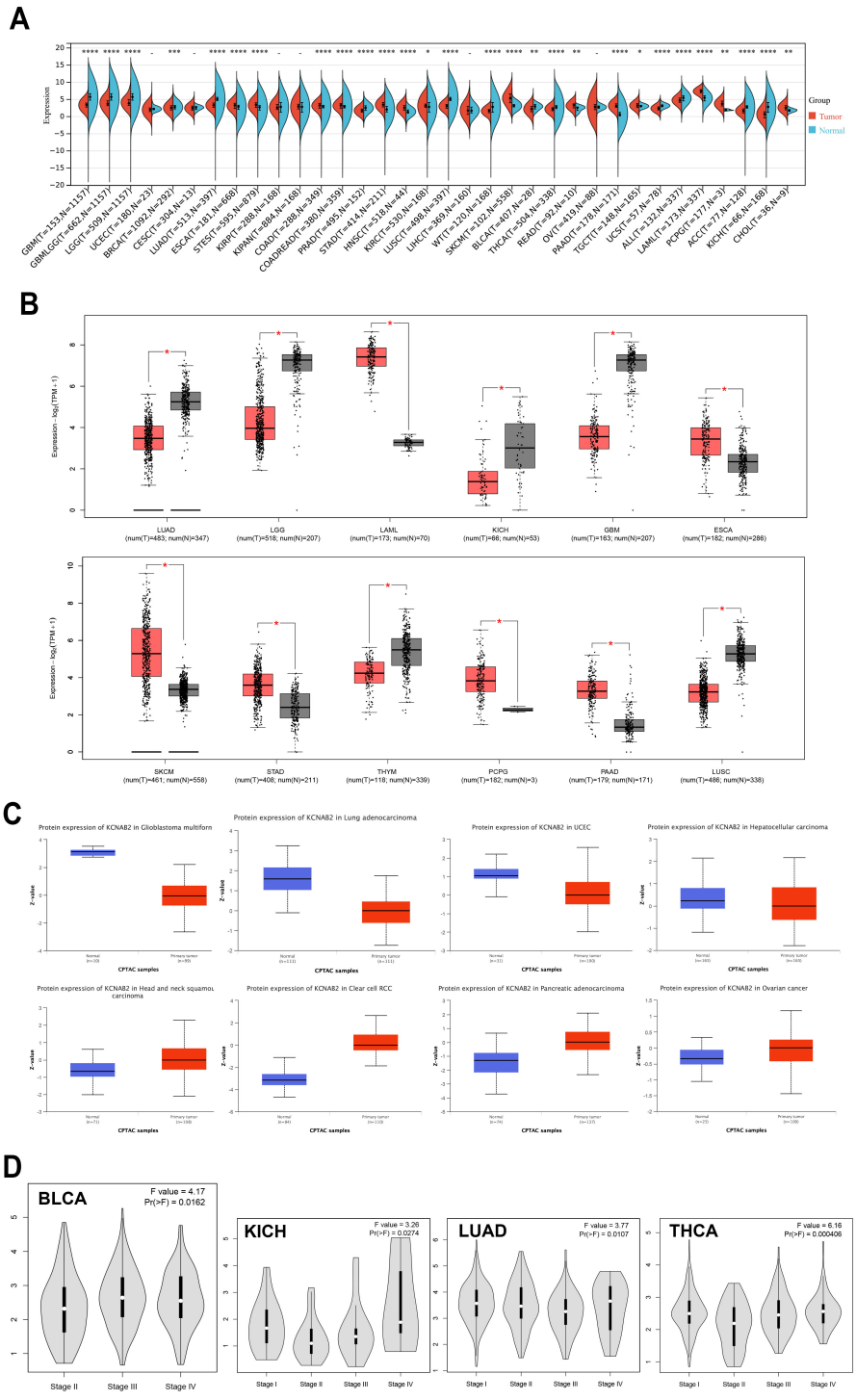


Figure 1

The expression levels of KCNAB2 in pan-cancer.

(**A**) KCNAB2 expression levels in different cancers from the TCGA database analyzed by the Sangerbox database. (**B**) KCNAB2 expression levels in different cancers and paired normal tissue in the GEPIA database. (**C**) KCNAB2 protein levels in different cancers in the UALCAN database. (**D**) KCNAB2 expression levels in different tumor stages in GEPIA2.0 database. (*p<0.05; **p<0.01; *** p<0.001; **** p<0.0001).

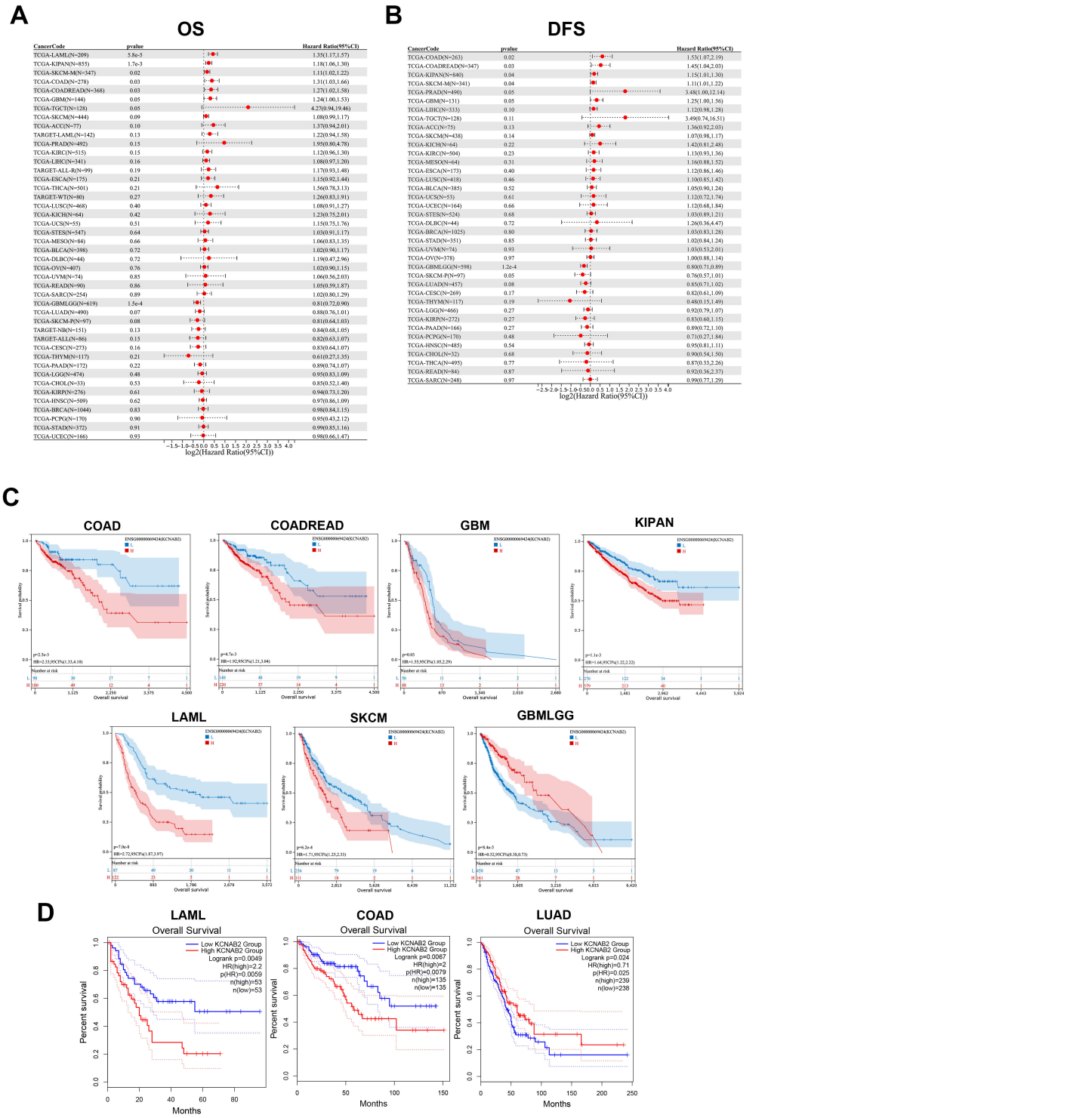


Figure 2

The prognosis value of KCNAB2 in pan-cancer.

(**A**, **B**) The forest plot indicated the correlations of KCNAB2 with overall survival (OS) and disease-free survival (DFS) in pan-cancer. (**C**, **D**) Kaplan-Meier analysis of the association between KCNAB2 expression and OS.

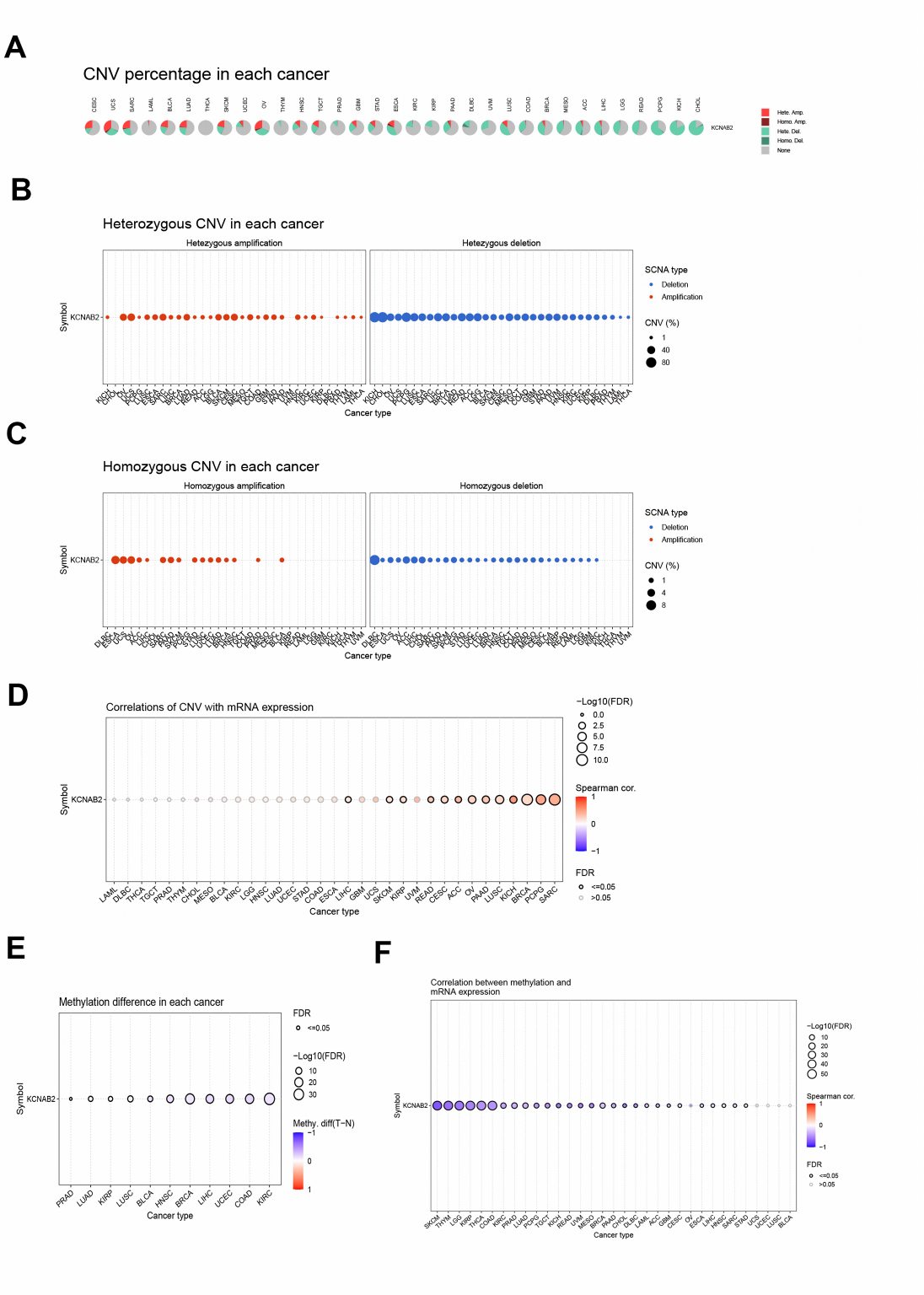


Figure 3

The CNV and DNA methylation of KCNAB2 in pan-cancer.

(**A**) The change frequency of CNV in KCNAB2 was showed by GSCA database. (**B**-**C**) The analysis of the Heterozygous/Homozygous CNV of KCNAB2 in pan-cancer. (**D**)The correlation of CNV with KCNAB2 mRNA expression in pan-cancer. (**E**) The differential methylation analysis of KCNAB2 in pan-cancer. (**F**) The correlation analysis showed that the methylation level of KCNAB2 was negatively correlated with mRNA expression

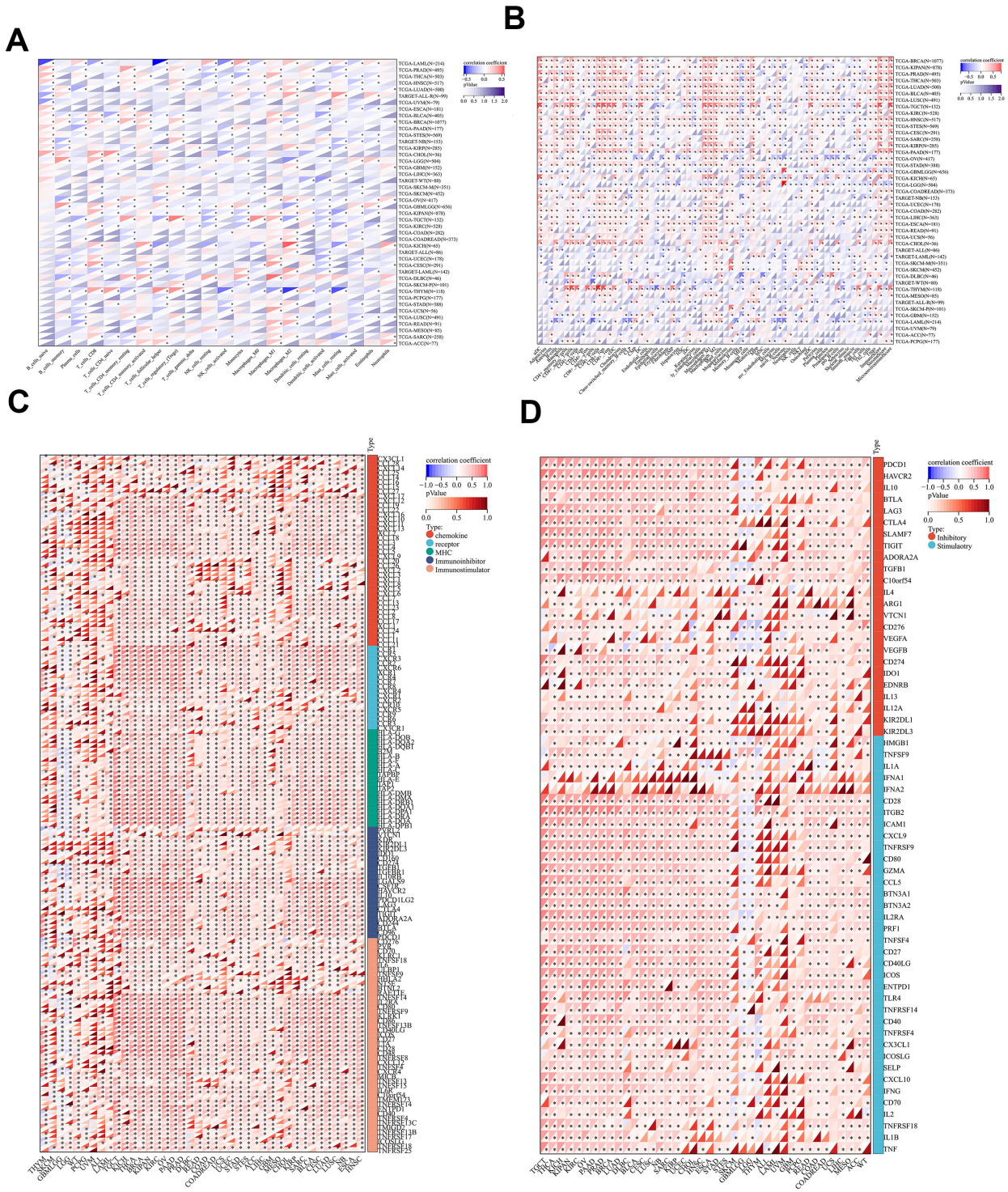


Figure 4

Correlation of KCNAB2 with the tumor immune microenvironment pan-cancer.

Relationship of KCNAB2 expression with immune cell infiltration analysis in pan-cancer by (**A**) CIBERSORT method, (**B**) xCELL method. (**C**, **D**) Relationship of KCNAB2 expression with immune-related genes and immune checkpoint genes. (*p<0.05)

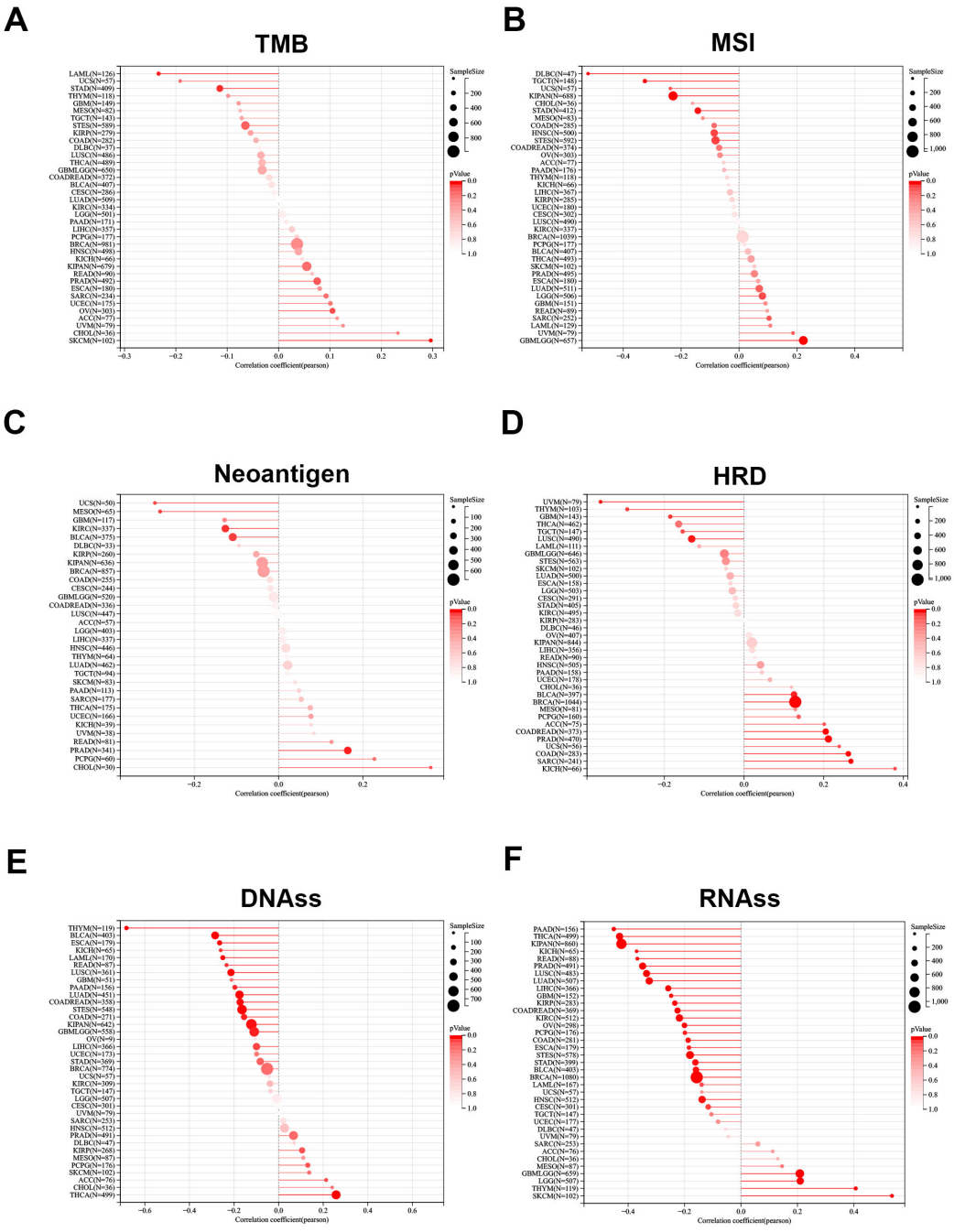


Figure 5

Relationship of KCNAB2 expression with TMB, MSI, Neoantigen, HRD, and cancer stemness in pan-cancer.

(**A**) Correlation between KCNAB2 expression and TMB. (B) Correlation between KCNAB2 expression and MSI. (**C**) Correlation between KCNAB2 expression and neoantigen. (**D**) Correlation between KCNAB2 expression and HRD. (**E**) Correlation between KCNAB2 expression and tumor stemness based on DNA methylation (DNAss). (**F**) Correlation between KCNAB2 expression and tumor stemness based on gene expression (RNAss).

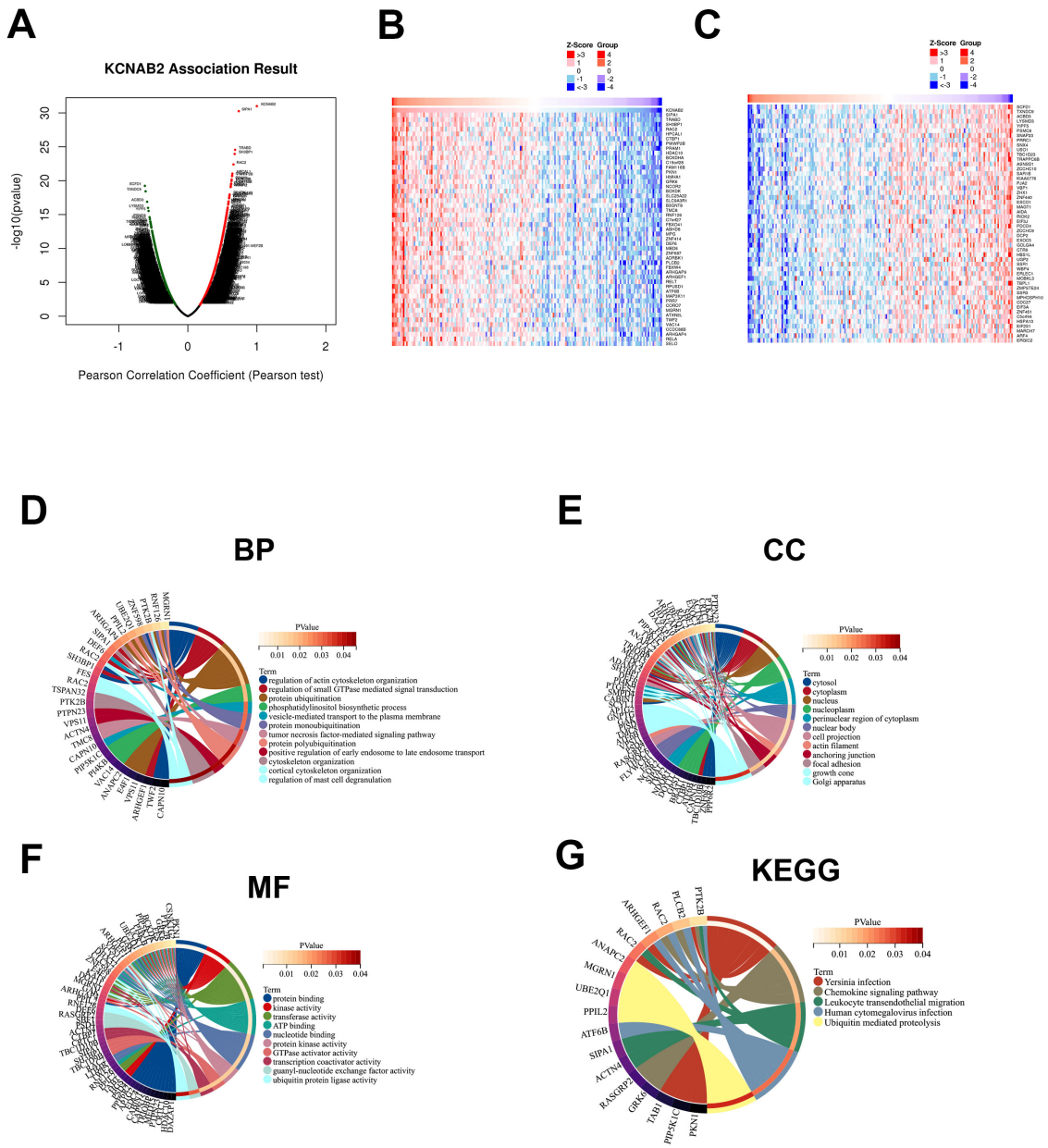


Figure 6

The analyses of KCNAB2-related genes in AML. (A) Genes with significantly high correlation with KCNAB2 in the LAML cohort. Heatmaps showing the enrichment patterns of the top 100 genes positively (50) (**B**) or negatively (50) (**C**) correlated with KCNAB2 expression of LAML in TCGA database. (**D**-**F**) The GO enrichment analysis was applied with the top 100 KCNAB2 positive related genes. (**G**) The KEGG enrichment analysis was used to analyze the top 100 KCNAB2 positive related genes.

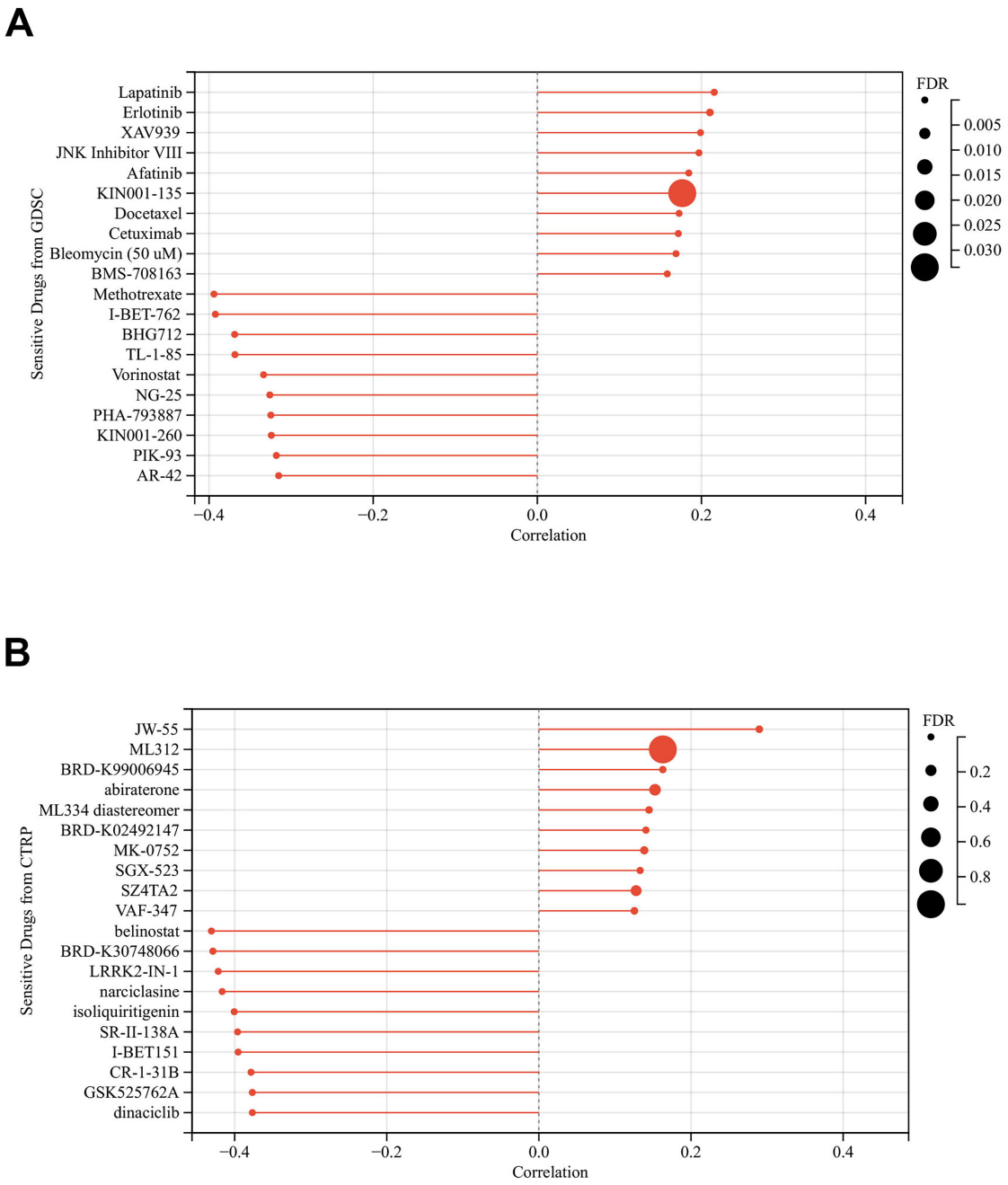


Figure 7

Drug sensitivity analysis based on KCNAB2 expression using the two different databases GDSC (A) and CTRP (B).

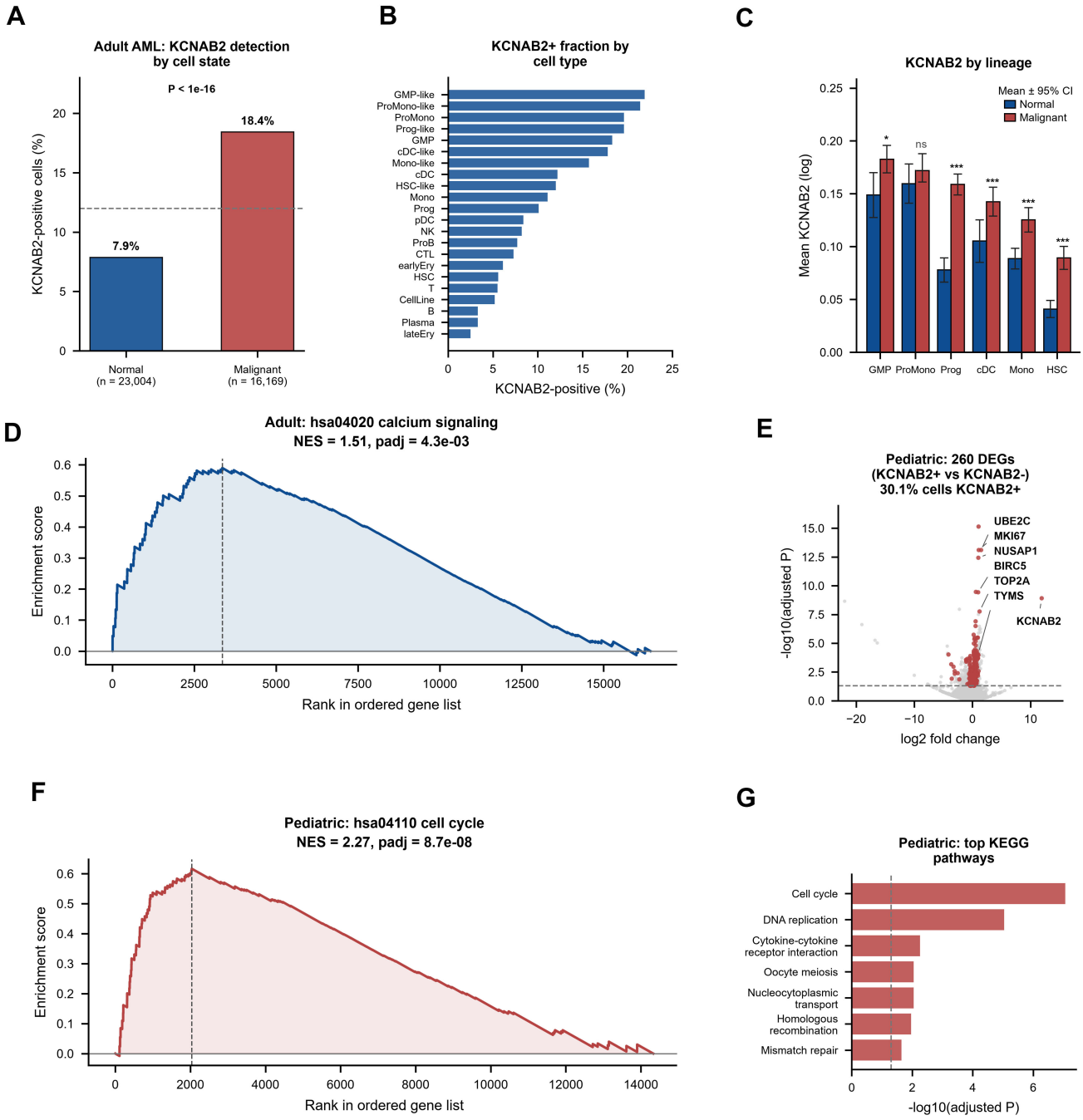


Figure 8

Single-cell KCNAB2 expression and KCNAB2-positive versus KCNAB2-negative comparison in adult and pediatric AML. (A) KCNAB2-positive cells among normal (n = 23,004) and malignant (n = 16,169) cells in GSE116256; dashed line, 12.0% overall; P, two-proportion z-test. (B) KCNAB2-positive fraction by cell type (GSE116256). (C) Mean log1p(KCNAB2) for normal versus malignant cells across six lineages; Wilcoxon FDR (*FDR<0.05, **FDR < 0.001, ns=not significant). (D) GSEA for hsa04020 calcium signaling in adult AML (NES =1.51, adjusted P=4.3×10⁻³). (E) Volcano plot of KCNAB2-positive versus KCNAB2-

negative cells in GSE154109 (30.1% positive); red points, FDR<0.05 (n=260). (F) GSEA for hsa04110 cell cycle (NES=2.27, adjusted P=8.7×10⁻⁸). (G) Top enriched KEGG pathways ranked by adjusted P (GSE154109); red bars, adjusted P < 0.05; dashed line, P=0.05.

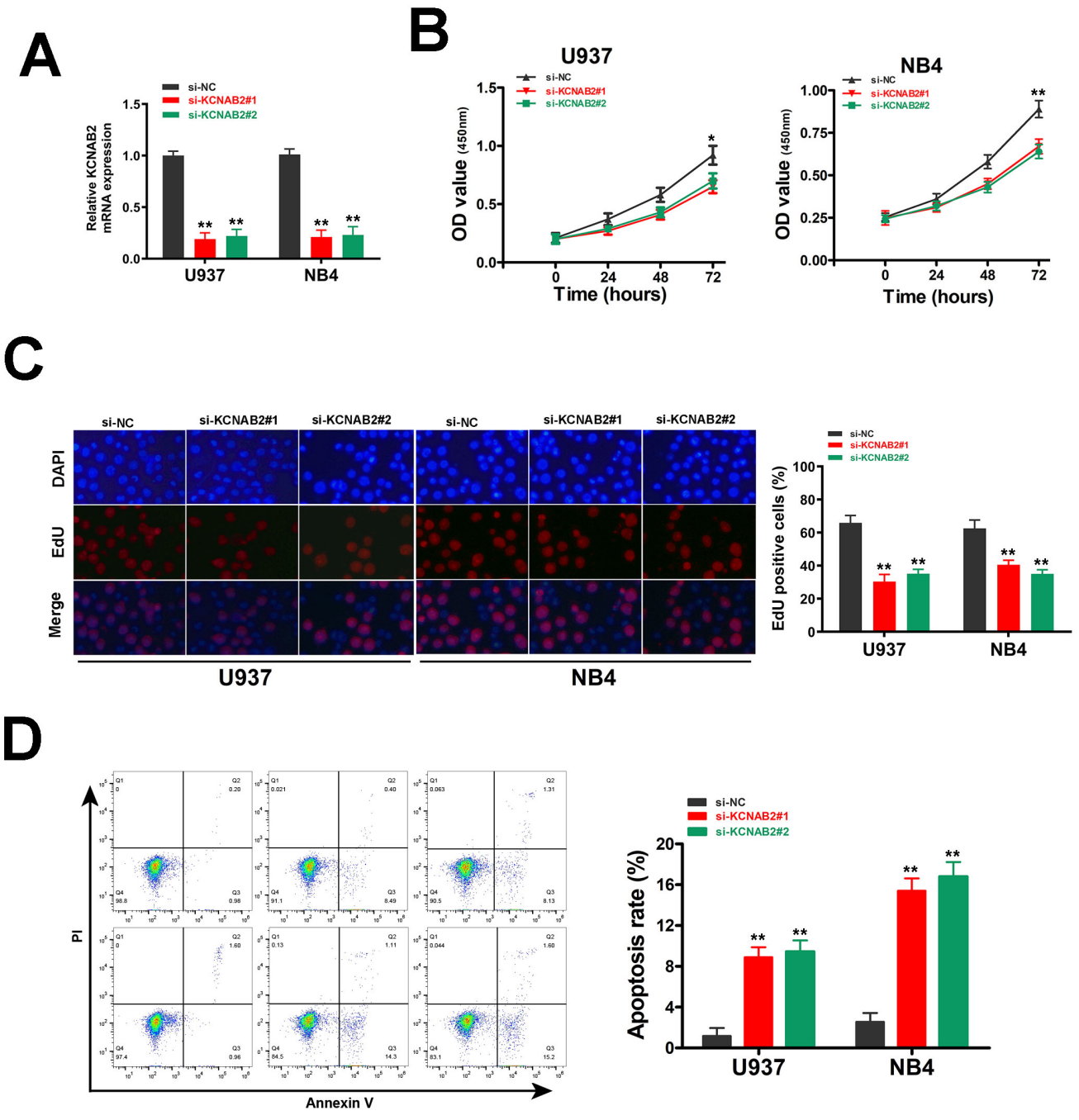


Figure 9

The biological functions of KCNAB2 in AML. (A) Relative mRNA expression of KCNAB2 in AML cells transfected with KCNAB2 siRNA. (B, C) Cell proliferation of AML cell was detected by CCK8 assay and EdU assay. (D) The apoptosis of AML cell was assessed by flow cytometry analysis. *p<0.05, **p<0.01.